

Research Article

## Biochars produced by slow carbonisation of three agricultural biomasses: physicochemical properties and potential for sustainable agro-environmental applications

**Komi Jean-Marcel AMEWOUAME\***

Laboratoire Chimie Organique et Sciences de l'Environnement (LaCOSE), Faculté des Sciences et Techniques (FaST), Université de Kara, Togo, B.P. 404, Kara

**Taba To'ora KAGA**

Eau et Environnement Limoges (E2Lim), UR 24133, ENSIL-ENSCI, Université de Limoges, 16 rue Atlantis 87068 Limoges Cedex, France

**SEGBEAYA Kwamivi N.**

Laboratoire Chimie Organique et Sciences de l'Environnement (LaCOSE), Faculté des Sciences et Techniques (FaST), Université de Kara, Togo, B.P. 404, Kara

\*Corresponding author. E-mail: marcelamewouame@gmail.com

### Article Info

<https://doi.org/10.31018/jans.v18i1.7261>

Received: October 12, 2025

Revised: February 28, 2026

Accepted: March 05, 2026

### How to Cite

AMEWOUAME, K. J.-M. *et al.* (2026). Biochars produced by slow carbonisation of three agricultural biomasses: physicochemical properties and potential for sustainable agro-environmental applications. *Journal of Applied and Natural Science*, 18(1), 452 - 465. <https://doi.org/10.31018/jans.v18i1.7261>

### Abstract

Agricultural by-products, such as cashew nut shells (CNS), sorghum stems (SS), and corn stems (CS), constitute unutilized waste. However, these by-products can be used to produce biochar, which improves soil structure and fertility while contributing to water retention and carbon stability. The objectives of this research were to produce biochars from these three biomasses and to evaluate the physico-chemical characteristics of the biochars obtained [yield, pH, macro and micronutrient content, electrical conductivity (EC), infrared analysis (FTIR), specific surface area (SBET), morphology (SEM), and CHNS/O content]. A total of eighteen biochar samples were obtained by varying the carbonisation temperature (350 and 400 °C) and residence time (30, 60, and 120 min) in a muffle furnace. At a fixed temperature, yield decreases with increasing residence time, surface area, pH, and electrical conductivity. Among the eighteen types of biochar, the one derived from corn stalks had an apparent specific surface area of (35.07 m<sup>2</sup>/g), followed by sorghum stalks (32.45 m<sup>2</sup>/g) and cashew nut shells (0.14 m<sup>2</sup>/g). The pH of the biochars is in the basic range (7.6–10.3). Furthermore, Krevelen's diagram reveals that biochars made from cashew nut shells are more stable in the long term, with the potential to persist for several centuries. These properties suggest that different types of biochar can be produced by adjusting production conditions and selecting biomass based on the soil characteristics in which it can be applied.

**Keywords:** Biomass, Biochar, Carbon sequestration, Soil amendment

### INTRODUCTION

In the face of the ever-increasing difficulties associated with soil degradation, climate change, and more broadly, the need for sustainable agriculture, biochar emerges as a long-term alternative to traditional soil amendments (Lehmann and Joseph, 2015). Biochar is a new scientific concept referring to a porous carbon-based solid produced at temperatures between 300 and 700 °C from lignocellulosic biomass residues by dry carbonisation or pyrolysis (Parmakoğlu *et al.*, 2023). Technologies for producing biochars have evolved. They have

evolved from open-air furnaces to more controlled systems such as fixed-bed, continuous or fluidised reactors, which allow the regulation of thermal parameters and the reproducibility of biochar properties. Biochar is widely recognised as an effective tool due to its multi-functional applications, including improving the physico-chemical properties of soils for effective fertilisation, sequestering carbon, and immobilising heavy metals and inorganic pollutants (Lehmann *et al.*, 2011). Its chemical and physical properties are strongly linked to the type of biomass used and the carbonisation conditions (Jindo *et al.*, 2014).

Carbonisation is important for identifying the most appropriate application of biochar in soil. Agricultural waste, such as biomass residues, is increasingly valued as a renewable raw material due to its high carbon content and its potential to produce biochar and bioenergy (Kwapinski *et al.*, 2010). Valorising these residues into biochars addresses the issue of sustainable management, avoiding open burning, reducing CO<sub>2</sub> emissions, and enriching the soil (Lehmann and Joseph, 2015). The temperature at which biochar is produced significantly affects its physicochemical properties (Ateş *et al.*, 2013). Biochar derived from relatively low-temperature carbonisation is characterised by a high content of volatile substances containing easily decomposable substrates, which promotes plant growth (Robertson *et al.*, 2012). Biochar has physicochemical properties that make it interesting for several energy, environmental, agricultural, and forestry applications. In the energy industry, it is like coal, and in agriculture and forestry, it is like organic matter (Allaire, 2013). The main interest in using biochar in soil today lies in its environmental sustainability benefits, as it is considered a new methodology for establishing a long-term carbon sink for atmospheric CO<sub>2</sub> in terrestrial ecosystems, while reducing the need for chemical fertilisers, which cause pollution (Rehrah *et al.*, 2014).

Furthermore, the transformation of biomass carbon into biochar carbon results in greater sequestration than open burning or direct biomass application (Lehmann *et al.*, 2006). Few studies have explored and compared the production of biochar from different agricultural residues at low carbonisation temperatures (<400°C) with varying carbonisation times. (Mukherjee *et al.*, 2022) examined the influence of residence time on yield and physicochemical properties at temperatures ranging from 400 to 600°C for 30 and 90 minutes, which improves biochar stability. However, this temperature variation exceeds 400°C, with only a small variation in residence time and no comparison of the properties of the biochars obtained under the same conditions. This study aimed to produce biochars at low temperatures by varying the carbonisation time with a variety of agricultural residues, and to compare their potential as soil conditioners and carbon stabilisers.

## MATERIALS AND METHODS

### Preparation of biochars

The sorghum and maize stalks, as well as the cashew nut shells, were dried in the sun for 3 days. They were then placed in an oven at 40 °C for 24 hours to reduce their residual moisture content, then cut into pieces no larger than 3 cm. The cashew nut shells (CNS) were carbonised in their natural form due to their high mechanical rigidity. This difference in particle size and geometry reflects the intrinsic physical properties of the

raw materials and can influence heat transfer and devolatilisation behaviour during carbonisation; this parameter was taken into account in the interpretation of the results. The Nabertherm L24/11 programmable muffle furnace (internal dimensions 230 x 250 x 200 mm) was used to carbonise the biomass in a static atmosphere (limited air) at a maximum temperature of 1100 °C. Carbonisation was carried out at final temperatures of 350 °C and 400 °C with residence times of 30, 60, and 120 minutes. A total of eighteen (18) biochars were produced and used in this study, derived from three different feedstocks: cashew nut shells (CNS), sorghum stalks (SS), and corn stalks (CS). The biochars were coded according to feedstock type, carbonisation temperature, and residence time. The furnace was preheated for 2 hours before each production cycle to reach a stable temperature. Each precursor was placed in a porcelain crucible. Table 1 summarizes the factors that influence biochar production.

After carbonisation at the desired temperature for the desired duration, the biochars were cooled in a desiccator at room temperature, ground in a mortar to a particle size of less than or equal to 1 mm, and stored in an airtight container. The objective was to produce biochars that are inexpensive, readily available, and can be produced at temperatures more easily attainable in real conditions using biomass. Furthermore, the main components of biomass decompose within the chosen temperature range. Notably, hemicellulose decomposes at temperatures between 220 and 315°C, cellulose at 315-400°C, and lignin at 160-900°C, depending on the biomass (Yang *et al.*, 2007).

### Immediate analysis

Immediate analysis primarily relies on determining moisture content, volatile matter content, ash content, and fixed carbon content. The moisture content of biomasses is obtained in an oven at 105°C according to the NF EN 14774-2 standard. The volatile matter content is obtained at 900°C for 7 minutes according to ISO 18123. The ash content is determined at 550°C in a muffle furnace until complete combustion according to ISO 18122. The fixed carbon content is determined by subtracting the sum of the ash and volatile matter content from 100.

### Analytical characteristics of the synthesised biochars

#### Mass yield

The mass yield represents the ratio of the mass of the biochar obtained to the mass of the dry shell used (Formula 1). All masses were measured using a high-precision balance from GOLDEN-METTLER USA

$$Y(\%) = \frac{\text{biochar mass}}{\text{dry shell mass}} \times 100 \quad (1)$$

### pH and electrical conductivity

The Sartorius pH meter was used to measure the pH of the different types of biochar. These biochars are produced as granules in a mortar. They are then introduced into distilled water at a 1:10 biochar:water ratio, as recommended by Singh *et al.* (2017). The mixture was homogenised by vigorous agitation for 30 minutes, followed by sedimentation for 10 minutes and filtration, and then the pH is measured. The electrical conductivity was measured in the same solution using a Thermo Scientific Orion Star A212/A329 conductivity meter.

### Concentration of macronutrients and micronutrients

#### Total nitrogen content

Total nitrogen content was determined using the Kjeldahl method (Dabin, 1965). The principle was based on the mineralisation of a 3 g sample with concentrated sulphuric acid and a catalyst to convert organic nitrogen into ammonium sulphate, followed by dilution and adjustment to an alkaline pH. The released ammonia is distilled into a 20 g/L boric acid solution in excess, then titrated with 0.02 N sulfuric acid to determine the ammonia bound by the boric acid, and the nitrogen content of the sample was calculated from the amount of ammonia produced. Formula 2 was used to determine the nitrogen content.

$$N_{tot} = \frac{1,401 \times T \times (V_1 - V_0)}{m} \times 100 \quad (2)$$

With T, the normalcy of the sulphuric acid solution;  $V_0$  the volume in millilitres of the sulphuric acid solution used for the blank test;  $V_1$  the volume in millilitres of the sulphuric acid solution used for the determination, and m the mass in grams of the sample.

#### Total phosphorus content

Phosphorus was dosed using the ceruleomolybdc method, which is based on the formation and reduction of a complex of orthophosphoric acid and molybdc acid. The reduction of phosphomolybdc acid results in a blue colour, the intensity of which is proportional to the amount of phosphorus present in the medium in question. One gram of the sample is calcinated at 500 °C for 5 hours, then dissolved in a 100 ml volumetric flask. To 4 ml of the solution, 2 ml of sulphomolybdate mixture and 5 ml of ascorbic acid were added, then the volume is made up to 20 ml with distilled water. The mixture is heated in a water bath at 85 °C for 10 minutes and the phosphorus is read using a UV-visible spectrophotometer at 650 nm. Standard solutions were prepared in sulfuric acid (1 N) from monopotassium phosphate ( $\text{PO}_4\text{H}_2\text{K}$ ). The phosphorus content is expressed in mg/100 g using formula 3:

$$P = \frac{lc \times V_{ext} \times Fd}{Pe} \quad (3)$$

where lc is the reading given by the spectrometer,  $V_{ext}$  is the volume of the sample taken for testing, Fd is the dilution factor, and Pe is the volume of the sample taken for testing.

#### Total sodium and zinc content

The total sodium and zinc content was determined by atomic absorption spectrometry (AAS) according to the standard NF EN ISO 6869, March 2002. Five grams of the sample were calcined, then dissolved in a 50 ml flask with nitric acid (0.05 M). Standard ranges were prepared and analysed by AAS to plot the calibration curves. The mineral concentrations are read and expressed in mg/100 g using formula 4.

$$P = \frac{C_{lue} \times V_r \times Fd}{Pe} \times \quad (4)$$

Where P is the mineral content (mg/100 g);  $C_{lue}$  the concentration read on the screen (mg/L);  $V_r$  the volume of recovery (l); and  $C_{lue}$  the sample weight (g).

#### Analysis by Fourier transform infrared spectroscopy (FT-IR)

Infrared spectra of twelve (12) biochars obtained during 30 and 120 minutes were recorded using a NICOLET iS5 Fourier transform infrared spectrometer with a spectral resolution of 4  $\text{cm}^{-1}$ . The baseline was established using a pellet composed of 150 mg of pure potassium bromide (KBr). For each analysis, the sample was prepared by homogenising 0.4 mg of biochar powder with 150 mg of KBr, then compressing the mixture into a tablet for analysis in the spectrophotometer. Table 2 shows the functions attributed to the different wave numbers.

#### Determination of the porous surface area by the BET method

The specific surface areas of the (12) biochars obtained at 30 and 120 minutes were measured using an automated sorptometer of the ASAP 2020 Micrometrics type at liquid nitrogen temperature (77K). The BET surface area calculation was performed using eight points on the adsorption curve at relative pressures of  $0.05 \leq P/P^0 \leq 0.30$ . Before analysis, the samples were degassed at 90°C for 30 minutes, followed by 200°C for 16 hours under vacuum using a turbo-molecular pump (vacuum level: 13  $\mu\text{bar}$ ).

#### Elemental analysis by CHNS/O analyzer

To determine the elemental chemical composition of the samples, 1 to 2 mg of sample was introduced in a tin boat and subjected to 'flash' combustion at 1000°C, releasing gases that undergo a treatment cycle

**Table 1.** Variation in biochar production factors

Biochars	Temperature (°C)	Carbonisation time (min)
CNS-350_30		30
CNS-350_60	350	60
CNS-350_120		120
CNS-400_30		30
CNS-400_60	400	60
CNS-400_120		120
SS-350_30		30
SS-350_60	350	60
SS-350_120		120
SS-400_30		30
SS-400_60	400	60
SS-400_120		120
CS-350_30		30
CS-350_60	350	60
CS-350_120		120
CS-400_30		30
CS-400_60	400	60
CS-400_120		120

-CNS denotes biochar derived from cashew nut shells; SS denotes biochar derived from sorghum stalks; CS denotes biochar derived from corn stalks

(oxidising, reducing, etc.) in a reactor tube and/or specific traps. The CHNS Flash Smart elemental analyser was used in this study. The treated gases are then separated using gas chromatography. The quantity of each compound is determined using a thermal conductivity detector (TCD). This analysis was performed on a total of 6 samples. The oxygen content was determined by calculation: subtracting the sum of the percentages of nitrogen (N), carbon (C), hydrogen (H), sulphur (S), and the ash content from 100 (Chung *et al.*, 2024).

**Analysis by scanning electron microscopy (SEM)**

The morphology of the samples was examined using a Hitachi TM3000 scanning electron microscope. A few milligrams of each biochar sample were pressed onto a carbon disc and then introduced into the microscope for observation.

**RESULTS AND DISCUSSION**

**Characterisation of biomass**

The immediate analysis of the three types of biomass focuses primarily on moisture content, volatile matter, ash content, and fixed carbon. Table 3 shows the results of the immediate analyses of the three types of biomass.

The analysis reveals that the cashew shells are composed of nearly 82.50% ± 0.99 volatile matter, 14.53% ± 0.34 fixed carbon, and 2.97% ± 0.08 ash. This composition is similar to that of cashew nut shells from Benin, which were evaluated at 81.6%, 15.8%, and 2.6% for volatile matter, fixed carbon, and ash content, respectively (Godjo, 2017). These values differ slightly from those of cashew nut shells from Nigeria, which have a composition of 65.21% volatile matter, 22.21% fixed carbon, and 2.75% ash (Kumar *et al.*, 2012). The moisture content of the sorghum stems is 2.56% ± 0.028. This value is significantly lower than the range reported in the literature, which spans 46.50% to 56.62% for the chemical and bioenergetic characterisation of sorghum agronomic groups (McKinley *et al.*, 2018). This variation could be explained by the type of sample and the time at which it was collected. The sorghum stems used in this study are collected after harvest and are therefore almost dry. Biomass containing more than 30% water is not suitable as a raw material (Tripathi *et al.*, 2016). Drying the raw material to a moisture content of 10 -15% is often necessary (Zabaleta *et al.*, 2018). A high ash content leads to poor combustion and disposal problems (Chen *et al.*, 2023). This is not the case for these biomasses, as when added to soil for carbon sequestration, it is desirable to have charcoal with less ash and more carbon (Chou, 2015). The sorghum and maize stems have a higher volatile matter content than the cashew nut shells, which could reduce the biochar's durability for long-term carbon sequestration.

**Table 2.** Vibration and wave numbers of spectra (FTIR) (Carrier *et al.*, 2012 and zwieten, 2010 and Gaskin *et al.*, 2008)

Wave number (cm <sup>-1</sup> )	Types of vibration
3400	Stretching vibration of O-H hydroxyl
2950	Stretching vibration of C-H bonds in
2850	Asymmetric stretching vibration of the C-H bonds of the CH <sub>2</sub> and CH <sub>3</sub> groups
1740-1720	Stretching vibration of aldehyde groups
1620 - 1650	Stretching vibration of C=C bonds in aromatic groups and C=O bonds in amide, ketone and quinone groups
1580 -1590	Asymmetric stretching vibration COO-
1460	Asymmetric deformation vibration of C-H bonds in CH <sub>3</sub> and CH <sub>2</sub> alkyl groups
1000 - 1100	Asymmetric stretching vibration Si-O-Si

**Table 3.** Immediate analysis of biomass

Biomass	CS	SS	CNS
Moisture (%)	2.53 ± 0,02	2.56 ± 0,03	7.51 ± 0,49
Volatile matter (%)	91.47 ± 0,68	90.49 ± 0,75	82.50 ± 0,99
Ashes (%)	5.13 ± 0,09	5.88 ± 0,12	2,97 ± 0,08
Fixed carbon (%)	3.4 ± 0,28	3.63 ± 0,64	14.53 ± 0,34
N <sub>tot</sub> (%)	0.48 ± 0,19	0.51 ± 0,09	0.31 ± 0,03
Na (mg/kg)	111 ± 1.02	157 ± 0.98	6079 ± 28.97
P <sub>tot</sub> (mg/kg)	1968 ± 4.68	2386 ± 5.10	2203 ± 4.55
Zn (mg/kg)	15.6 ± 0.57	56.9 ± 2.31	10.3 ± 0.52

CNS : cashew nut shells; SS : sorghum stalks ; CS : corn stalks

tion, but this can be corrected by increasing the quantity per unit area. Nevertheless, this increase in volatile matter will provide a porous structure (Mohan *et al.*, 2006). and nutrients to improve the activity of soil microorganisms (Joseph, 2012). Furthermore, the high fixed carbon content can be explained in part by the intrinsic chemical composition of the raw material and by physical effects related to particle size (Di Blasi, 2008). In view of the results of the immediate analyses of the three biomasses, they are predisposed to being precursors to produce biochar.

### Physicochemical characteristics of biochars

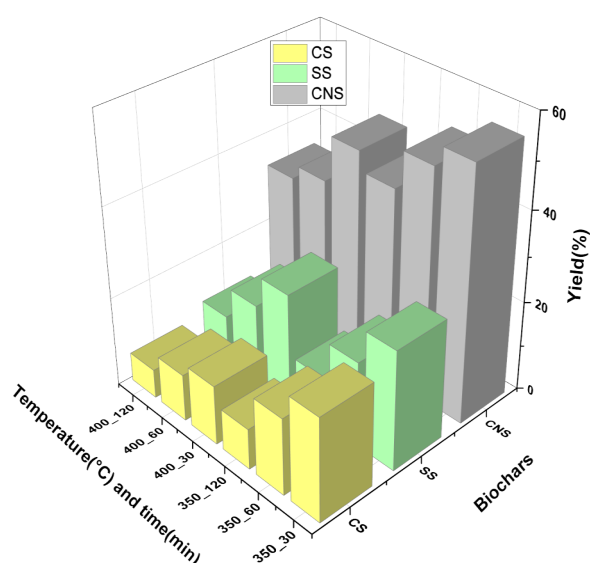
#### Mass production yield

It is necessary to know the biochar production yield to assess the availability of raw materials if this technology were to be transferred to an industrial setting. The production yield of biochars was determined for the three biomasses, namely the cashew nut shells (CNS), sorghum stems (SS), and corn stems (CS). Fig. 1 illustrates the yield of the different biochars. The ranking of

yields gave CNS (33.24 – 55.61) > SS (16.7 – 26.51) > CS (9.05 – 22.96). The high yield of biochar from cashew nut shells could be explained by their rigidity and by the apparent density resulting from the shells being arranged compactly in the crucibles, creating a specific thermal microenvironment that may affect heat penetration. Values ranging from 46.2 to 35.9% and from 37.8 to 30.3% by mass at temperatures of 350 °C and 400 °C were found by (Kadjo *et al.*, 2024) to extract the oil. Low-temperature carbonisation yields more biochar and volatile matter than high-temperature carbonisation (Jindo *et al.*, 2014). This can be observed for these biomasses: the two temperature conditions (350 °C and 400 °C), despite being low, show differences due to temperature variation and different residence times. Furthermore, the type of raw material also affects biochar yield. For the same residence time, yields differ across biomass types at different temperatures. They decrease respectively for cashew nut shells, sorghum stems, and corn stems. Similar findings were reported by Khater *et al.* (2024), who observed a decrease in biochar production yields when the temperature varied from 400 to 800°C with biomasses such as rice straw, wood chips, sugarcane residue, and tree leaves, due to increased combustion rates. They attribute this to variations in the lignin and cellulose content of the biomass. Carbonisation of all biomass types resulted in greater biochar production at lower carbonisation temperatures. It should be noted that the differences observed in yield between biochar derived from cashew nut shells and that derived from stems cannot be attributed exclusively to the chemical composition of the raw material, but also to the larger particle size of CNS, which could, however, affect the transfer kinetics, potentially contributing to the variations observed (Di Blasi, 2008).

#### pH of biochars

The pH of biochar is important to know, as it may influence soil pH. The pH ranking is SS (9.23–10.28) > CS (9.26–10.05) > CNS (7.56–9.13). The lowest value is that of the carbonised cashew nut shells at 350°C for

**Fig. 1.** Mass yield of biochar production

30 minutes (CNS-350\_30), which is probably due to the presence of acidic cashew oil (Godjo *et al.*, 2015). The highest value is obtained with SS-400\_120. Basic pH values (pH > 9) were observed for biochars derived from corn stover. Fig. 2 shows the pH of the different biochars. Most biochars used for soil amendment are alkaline (Mukherjee *et al.*, 2014). However, pH values ranging from 3 to 12 have been reported in the literature (Mukherjee *et al.*, 2014;). During carbonisation, acidic functional groups are eliminated, and salts of alkaline and alkaline-earth metals are enriched (Fuentes *et al.*, 2010). These salts, which can be carbonates or silicates, give biochars considerable alkalinity (Vassilev *et al.*, 2013). However, this depends on the raw material and the cooking process (Xie *et al.*, 2015). A substantial increase in pH occurs at higher temperatures due to the increased relative concentration of non-carbonised inorganic elements in the raw materials.

### Conductivity

Conductivity is a parameter required by the International Biochar Initiative (IBI) that indicates the biochar's ability to conduct electricity. It is based on the principle that solutions with high salt concentrations have a greater ability to conduct electricity (Singh *et al.*, 2017). The highest value was obtained with biochar from cashew nut shells, ranging from 128 to 730  $\mu\text{S}/\text{cm}$  depending on the production conditions, and could lead to an increase in soil salinity, requiring appropriate dosing to protect sensitive crops (Beesley *et al.*, 2011). Biochars made from sorghum stalks had the lowest conductivity, ranging from 1.15 to 4.565  $\mu\text{S}/\text{cm}$ , as shown in Fig. 3. According to Joseph *et al.* (2010), biochar conductivity depends on the amount of salts it contains, and high biochar application rates in the soil can harm sensitive plants. Biochar salinity can therefore be eval-

uated by electrical conductivity, indicating that the capacity of plants to extract water from their environment depends not only on matric potential but also on the osmotic potential created by salinity (Chou, 2015). The electrical conductivity of biochars increases with temperature and carbonisation time. The highest values are obtained with biochar from cashew nut shells, ranging from 128 to 730  $\mu\text{S}/\text{cm}$  depending on the production conditions. Biochars made from sorghum stems showed the lowest conductivity of the three biochars. (1.15 – 4.565  $\mu\text{S}/\text{cm}$ ). This difference could be explained by the initial composition of the biomass, which is rich in basic cations ( $\text{K}^+$ ,  $\text{Ca}^{2+}$ ), which concentrate in the biochar after carbonisation (Lehmann and Joseph, 2015).

### Macro and micronutrient content

The macro and micronutrient content of biochars is an important factor in their agronomic value. The nutrients that have been determined are mainly total nitrogen, total phosphorus, sodium and zinc. Tables 4 and 5 illustrate the variations of these different minerals. For the three types of biochar at 350 °C, the total nitrogen content ranges from 0.65 to 1.41%. This small variation could be explained by nitrogen volatilisation during carbonisation. Therefore, biochars cannot be considered as nitrogen fertilisers (Chou, 2015). Rather, they can be considered organic amendments that improve soil structure and cation exchange capacity when incorporated. The nitrogen content obtained is consistent with studies in the literature on various types of biomasses, including hardwoods, softwoods, non-woody materials, and others, whose nitrogen content falls within the range of (0.21 to 5.71) (Chou, 2015). The sodium content ranges from 11,460 to 30,736 mg/kg. Biochar derived from corn stalks indeed has an extremely high

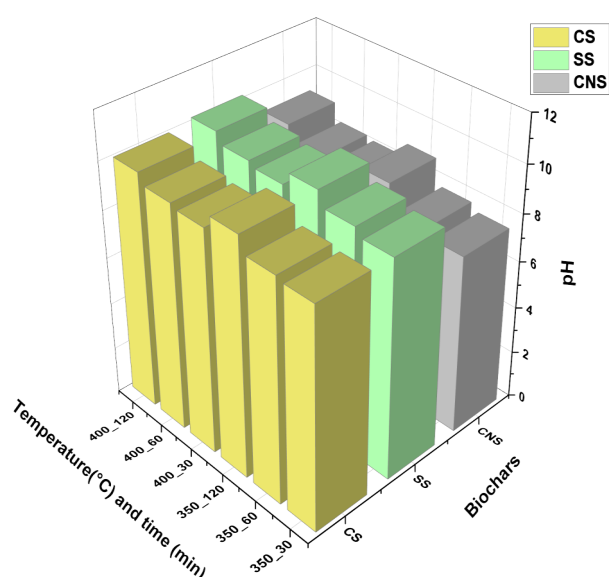


Fig. 2. pH of different types of biochars

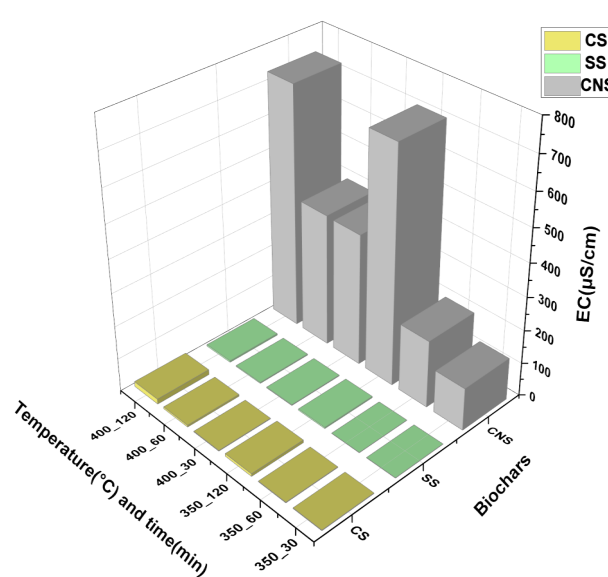


Fig. 3. Electrical conductivity of different types of biochar

**Table 4.** Variation in mineral content at 350°C as a function of residence time

Biochars	N <sub>tot</sub> (%)	Na <sub>tot</sub> (mg/kg)	P <sub>tot</sub> (mg/kg)	Zn <sub>tot</sub> (mg/kg)
CNS-350_30	0.83 ± 0.01	11460.7 ± 54.3	692.9 ± 0.14	7.26 ± 0.04
CNS-350_60	1.00 ± 0.04	15786.8 ± 70.5	715.3 ± 2.75	9.26 ± 0.05
CNS-350_120	1.04 ± 0.03	18556.9 ± 165	681.7 ± 0.65	10.77 ± 0.03
SS-350_30	0.69 ± 0.01	24028.7 ± 70	421.7 ± 0.56	6.26 ± 0.09
SS-350_60	0.65 ± 0.04	18973.6 ± 141	428.4 ± 1.83	6.75 ± 0.28
SS-350_120	0.72 ± 0.15	30736.3 ± 213	491.5 ± 1.62	10.49 ± 0.02
CS-350_30	1.08 ± 0.02	21253.57 ± 67	519.8 ± 0.42	33.215 ± 0.05
CS-350_60	1.41 ± 0.05	28850.4 ± 0.01	531.2 ± 0.67	33.69 ± 0.04
CS-350_120	1,37 ± 0.01	29767.9 ± 70	564.2 ± 0.35	35 ± 0.05

total sodium content (30,000 mg kg<sup>-1</sup>), and an agronomic risk assessment must account for soil salinity and sodicity thresholds. Soil salinity is generally expressed in terms of electrical conductivity, with values above 4,000 μS cm<sup>-1</sup> considered moderately saline and potentially restrictive for many crops, and values above 8,000 μS cm<sup>-1</sup> considered highly saline. Crop yield response models, such as the Maas-Hoffman model, indicate that salt concentrations above threshold levels result in significant yield reductions. Exchangeable sodium percentages above 15% and sodium adsorption ratios above are widely used as agronomic indicators of sodicity risk, which can adversely affect soil structure and plant growth. Therefore, despite the high total Na content of biochar, its practical risk of salinity and sodicity depends on the amount of sodium that becomes soluble and exchangeable in the soil environment rather than the total element concentration alone (Breker, 2016; Araujo *et al.*, 2024). The fact that CNS had the lowest ash content confirms that ash represents total mineral matter and may not correlate with the concentration of a specific element. The Na concentration in CNS biochars could be attributed to the biomass's initial composition and to concentration effects during carbonisation (Evans *et al.*, 2017). Increased nitrogen content (up to 1.58%) at 400°C, specifically for corn stalks, could suggest the formation of aromatic structures containing nitrogen, which would promote long-term stability and resistance to microbial degradation in the soil (Lehmann and Joseph, 2015). At 400°C, the phosphorus content varies from 468.36 to 884.75 mg/kg. The maximum value is obtained with biochar derived from cashew nut shells (CNS), followed by biochars derived from corn stems (CS) and sorghum stems (SS). This shows that the carbonisation temperature and the nature of the biomass influence the phosphorus content of biochars. Some biochars can therefore be used as a phosphorus amendment in soils and potting mixes. Unlike nitrogen, biochars rich in phosphorus may be restricted in certain applications, such as water filtration or repeated high doses in agricultural fields (Chou, 2015). Biochars obtained from cashew nut shells, sorghum, and maize stalks show a general ten-

dency for increased nitrogen (N), phosphorus (P), and zinc (Zn) content with increased carbonisation time. This increase could indicate a progressive concentration of nutrients due to increased evaporation of volatile compounds at prolonged temperatures and times (Enders *et al.*, 2012). The high values obtained from biochars from cashew nut shells are explained by the presence of mineral salts that concentrate after carbonisation, which is correlated with the high conductivity of biochars from cashew nut shells.

To better assess the effect of carbonisation, the elemental composition of the raw biomass was also determined (Table 3). The nitrogen, phosphorus, sodium and zinc contents varied according to the type of biomass, ranging from 0.31 to 0.51%, 1968 to 2386 mg/kg, 111 to 6079 mg/kg and 10.3 to 56.9 mg/kg, respectively. Comparison with biochars shows that carbonisation concentrates these elements, mainly through the loss of volatile matter and water. However, several studies indicate that the nutrients in biochar are not always immediately available to plants, as they are often bound to aromatic structures or solid mineral phases. Nevertheless, they can contribute to soil fertility through slow release and improved nutrient retention (Lehmann and Joseph, 2015). Aqueous extraction and soil-biochar incubation experiments show that most phosphorus and nitrogen remain in the solid phase (Mukherjee and Zimmerman, 2013), while aromatised nitrogen limits rapid mineralisation, indicating that biochar acts primarily to retain existing nutrients in the soil rather than as a direct source (Singh and Cowie, 2010).

#### **Spectroscopic responses in infrared with Fourier transform Infrared spectroscopy (FTIR)**

Infrared spectroscopy with Fourier transform (FTIR) is a tool for identifying functional groups in biochars (Keiluweit *et al.*, 2010). It highlights the structural changes induced by carbonisation, such as the gradual loss of labile oxygenated functionalities and the formation of more condensed aromatic structures, providing essential information on the chemical stability and surface reactivity of biochars (Chen *et al.*, 2011). Furthermore, it enables the evolution of characteristic

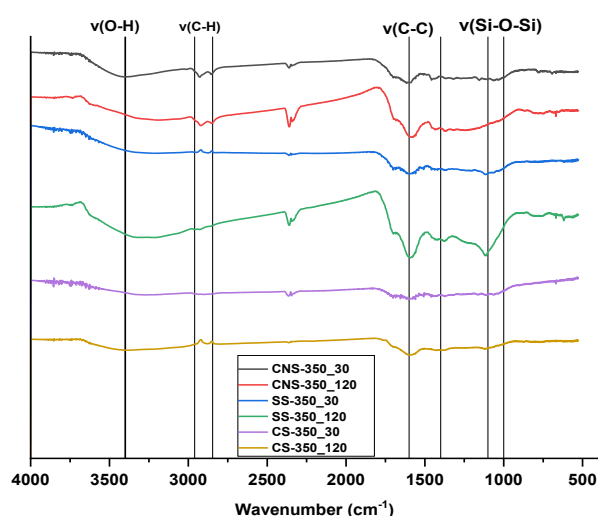
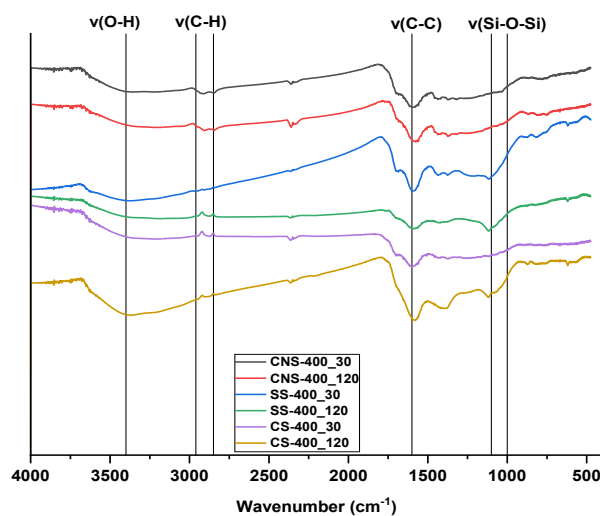
**Table 5.** Variation in mineral content at 400°C as a function of residence time

Biochars	N <sub>tot</sub> (%)	Na <sub>tot</sub> (mg/kg)	P <sub>tot</sub> (mg/kg)	Zn <sub>tot</sub> (mg/kg)
CNS-400_30	0.88 ± 0.06	18005.7 ± 141	883.9 ± 0.14	11.36 ± 0.42
CNS-400_60	1.02 ± 0.06	18066.5 ± 57	884.8 ± 1.13	11.61 ± 0.03
CNS-400_120	1.34 ± 0.03	19347.1 ± 165	864.9 ± 0.75	12.37 ± 0.03
SS-400_30	0.61 ± 0.1	26899.2 ± 563	468.3 ± 4.03	9.48 ± 0.09
SS-400_60	0.66 ± 0.04	24794 ± 215	482.7 ± 3.39	10.18 ± 0.01
SS-400_120	0.69 ± 0.01	32293.9 ± 717	686.1 ± 0.89	15.14 ± 0.12
CS-400_30	1.43 ± 0.15	19745.7 ± 6.73	532.9 ± 0.67	30.32 ± 0.28
CS-400_60	1.45 ± 0.01	31151.5 ± 1414	686.3 ± 0.64	34.63 ± 0.06
CS-400_120	1,58 ± 0.03	47317.7 ± 39	574.7 ± 1.30	36 ± 0.01

bands to be linked to the agronomic and environmental properties sought, such as carbon sequestration and cation exchange capacity (Lehmann and Joseph, 2015). Figs. 4 and 5 show the spectra obtained at 350 and 400 °C for biochars alone, after 30 and 120 minutes, to highlight the differences.

Fig. 4 shows the spectra of the different biochars obtained at 350 °C with carbonisation times of 30 and 120 minutes. The band at 3400 cm<sup>-1</sup> corresponds to the stretching vibration of the hydroxyl group (O-H), indicating the presence of hydroxyl groups and possible residual moisture (Kuligiewicz *et al.*, 2015). These bands are more pronounced for SS-350\_30 and CS-350\_120 and could increase their cation exchange capacity (Tomczyk *et al.*, 2020). Between 2960 and 2850 cm<sup>-1</sup>, a weak vibration of elongation of the aliphatic group (C-H) is observed, which is characteristic of a low degradation of the aliphatic chains in the biochars. The band around 1600 cm<sup>-1</sup> corresponds to a vibration of elongation of the aromatic (C=C) bond or aromatic cycles. A weak response is observed at 30 min and is slightly more pronounced at 120 min, which could indicate the formation of aromatic structures and, consequently, the onset of stability (Parikh *et al.*, 2014). These bands are

more pronounced in the SS-350\_120 and CS-350\_120 than in the biochars from cashew nut shells. This could be explained by the fact that cashew nut shells contain a lignocellulosic wall and an oil containing phenol, which undergoes dehydration and decarboxylation at temperatures between 300 and 400°C, resulting in a composite spectrum with broad bands rather than fine ones (Cruz, 2024). The band between 1100 and 1000 cm<sup>-1</sup>, specific to SS-350\_120, corresponds to the elongation vibration of the (Si-O-Si) group, indicating the presence of ash during carbonisation. Similar findings were reported by Qian and Chen (2013) when biochars were produced from rice and palm kernel husks by carbonisation at 350 and 500°C, and they estimated the vibration at 1091 cm<sup>-1</sup> to be due to aliphatic C-O or alcohol C-O stretching [48]. This shows that the duration of carbonisation and the nature of the biomass influence the different surface functions. Fig. 5 illustrates the spectra of the biochars obtained at 400 °C for 30 and 120 minutes. Increasing the carbonisation time from 30 to 120 minutes resulted in a slight decrease in the stretching vibration of the hydroxyl groups at 3400 cm<sup>-1</sup>, except for the biochars obtained from cashew nut shells, which could be explained by the presence of the

**Fig. 4.** Spectra of biochars obtained at 350°**Fig. 5.** Spectra of biochars obtained at 400°C

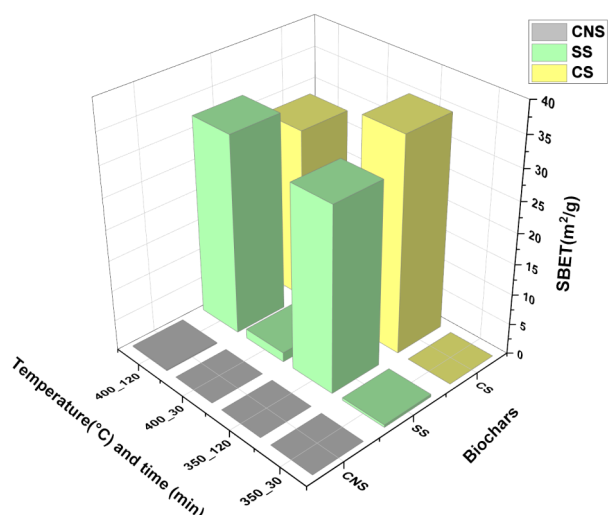


**Fig. 6.** Specific surface areas of biochars

condensate (the oil it contains). The band around  $1600\text{ cm}^{-1}$  corresponds to the stretching vibration of the (C=C) bond of the aromatic group. This can be seen in the cashew nut shells. This observation can be attributed to the typical aromatic structures of lignin, as cashew nut shells are rich in lignin (McCall *et al.*, 2025). The high electrical conductivity of CNS-400\_120 ( $730\text{ }\mu\text{S/cm}$ ) is correlated with a clear peak at  $1400\text{ cm}^{-1}$ , characteristic of soluble salts. This absence could be explained by the fact that the salts present do not induce a change in the dipole moment, a condition for a vibrational mode to be observed (Hsu, 1997). SS-400\_120 also shows an unclear peak at  $1600\text{ cm}^{-1}$ , characteristic of medium resistance to microbial degradation (Keiluweit *et al.*, 2010). According to Zhao *et al.* (2024), the band around  $2900\text{ cm}^{-1}$  decreases gradually with increasing carbonisation temperature and is attributed to dehydration or decarboxylation reactions, leading to the rupture of aliphatic chains. These changes are not very noticeable in Figs. 4 and 5 due to the low carbonisation temperatures (350 and  $400^\circ\text{C}$ ). This is corroborated by Tomczyk *et al.* (2020), who state that at low temperatures, biochar still contains oxygenated functions such as carboxyl, lactones, and phenols, which have not yet been completely deoxygenated. In summary, it is noted that the nature of the biomass, the increase in carbonisation temperature and the residence time influence the quality of the biochars produced.

### Specific surface areas of biochars

A total of 12 biochars derived from cashew nut shells (CNS), sorghum stalks (SS), and corn stalks (MS) were carbonised at 350 and  $400^\circ\text{C}$  for 30 and 120 minutes, respectively, and analysed to determine their specific surface areas.  $\text{N}_2$  adsorption isotherms at 77 K were measured using the BET method over  $0.05 \leq P/P^\circ \leq 0.30$ . The BET constants were negative ( $C < 1$ ), indicat-

ing that the BET model assumptions are not strictly met; therefore, the calculated surface areas are apparent values and should be interpreted with caution. This corresponds to type III isotherms, typical of materials with macroscopic pores (Hwang and Barron, 2011). Fig. 6 shows the apparent specific surface area of biochars. The apparent surfaces varied slightly for most samples. From 28-35  $\text{m}^2/\text{g}$  for samples SS-350\_120, SS-400\_120, and CS-400\_120. Short carbonization times (30 min) resulted in minimal pore development, while longer times (120 min) increased apparent pore formation. The dense, lignin-rich structure of CNS promoted tar formation and pore blockage, resulting in very low apparent surfaces, while the fibrous, low-density structure of SS facilitated partial pore development despite a higher ash content (Leng *et al.*, 2021). The highest apparent surface areas were  $35.07\text{ m}^2/\text{g}$  for SS-350\_120 and  $32.44\text{ m}^2/\text{g}$  for SS-400\_120, indicating partial macropore development. These biochars can nevertheless improve soil water retention and nutrient availability (Glaser *et al.*, 2002).

### Properties of biochar for storing carbon in the soil

Given the results obtained for specific surfaces, only six biochars carbonised for 120 minutes were analysed to determine their carbon, hydrogen, nitrogen, sulphur and oxygen content. These contents provide information on chemical composition, stability and carbon sequestration potential (Spokas, 2010). Table 6 shows the content of the various constituent elements. It can be seen that the biochars obtained at 350 and  $400^\circ\text{C}$  for 120 minutes have a high carbon content of 59.18% - 73.81%, followed by oxygen content of 15.28% - 24.49%. Hydrogen ranging from 2.37% to 4.66%, nitrogen varying from 0.44% to 1.8% and sulphur varying from 0% to 0.53%. The raw CHNS/O data do not allow for a direct assessment of the stability of the different biochars, so it is necessary to calculate the H/Corg ratio, which reflects aromaticity and the degree of condensation, and then the O/Corg ratio, which indicates polarity and surface oxidation.

The International biochar initiative (IBI) and the European biochar certificate (EBC) recognise these ratios. Thus, a low H/Corg ratio ( $< 0.7$ ) and an O/Corg ratio ( $< 0.4$ ) are recognised by EBC (2022) as criteria for the long-term stability of biochar. Consequently, the CHNS/O content can be used to certify the quality and sequestration function of biochars. Table 7 shows the different atomic ratios. The H/Corg ratio can be used to assess biochar stability and, consequently, its sequestration capacity.

The stability of biochar is important for two reasons: firstly, it determines how long the carbon applied to the soil in the form of biochar will remain in the soil and contribute to mitigating climate change; secondly, it determines how long biochar will continue to benefit the

**Table 6.** CHNS/O content of biochars

Biochars	N (%)	C (%)	H (%)	S (%)	Ash content (%)	O (%)
CNS-350_120	0.78 ± 0.04	71.94 ± 0.45	4.66 ± 0.15	0	5.29 ± 0.35	17.33 ± 0,47
CNS-400_120	0.44 ± 0.62	73.81 ± 1.52	4.23 ± 0.13	0	6.24 ± 0.26	15.28 ± 1.64
SS-350_120	0.76 ± 0.07	62.40 ± 1.73	2.77 ± 0.16	0.42 ± 0.05	10.49 ± 0.67	23.16 ± 1.73
SS-400_120	0.87 ± 0.03	59.18 ± 0.98	2.47 ± 0.02	0.53 ± 0.02	14.38 ± 0.51	22.57 ± 0.98
CS-350_120	1.80 ± 0.02	60.01 ± 0.40	2.37 ± 0.05	0.08 ± 0.01	11.25 ± 0.38	24.49 ± 0.4
CS-400_120	1.69 ± 0.02	59.35 ± 2.68	2.45 ± 0.23	0.1 ± 0.07	15.98 ± 0.64	20,43 ± 2.69

**Table 7.** Durability and persistence properties in soil of different types of biochars

Biochars	H/C	O/C
CNS-350_120	0.78 ± 0.03	0.18 ± 0.01
CNS-400_120	0.69 ± 0.02	0.16 ± 0,01
SS-350_120	0.53 ± 0.03	0.28 ± 0.02
SS-400_120	0.5 ± 0.01	0.29 ± 0.01
CS-350_120	0.47 ± 0.01	0.3 ± 0;00
CS-400_120	0.5 ± 0.03	0.26 ± 0.04

soil and plants (Lehmann *et al.*, 2006). It should be noted that an increase in temperature is inversely proportional to the H/Corg ratio, except for corn stalk biochars, which may be explained by the removal of surface polar functional groups and an increase in aromatic carbon (Cantrell *et al.*, 2012). Consequently, biochars produced at higher temperatures would be less polar, exhibit greater stability and aromaticity, and thus show a more hydrophobic character (Nguyen *et al.*, 2018). According to the International biochar initiative (IBI), the term 'biochar' only applies to carbon residue if the H/Corg ratio is less than 0.7. With the exception of CNS-350\_120, whose H/Corg ratio is slightly above the threshold (0.78), all biochars obtained after 120 minutes have an H/Corg ratio below 0.7, indicating good aromatisation, stability, and structure (McIntosh, 2013). They are therefore relatively recalcitrant. The O/Corg ratio ranges from 0.16 to 0.30. As with the H/Corg ratio, the O/Corg ratio decreases with increasing carbonisation temperature. In addition, biomass-derived materials generally contain labile and recalcitrant oxygen fractions; the former are quickly lost after initial heating, while the latter are retained in the final biochar (Rutherford *et al.*, 2012). It should be noted that the IBI gives priority to the H/Corg ratio, unlike the EBC, which also takes into account the O/Corg ratio. Based on the EBC (2022) requirements, all biochars have an O/Corg ratio of less than 0.4, suggesting high aromatic condensation and therefore stability. To find a compromise

between the two, we turn to Van Krevelen's diagram, illustrated in Fig. 7. This diagram aims to assess the degree of carbonisation by estimating the stability and persistence of biochar (Spokas, 2010). It is also a graphical tool often used to characterise the chemical stability of biochars and, therefore, their ability to sequester carbon. The diagram reveals that biochar is more stable when the H/Corg and O/Corg ratios decrease (IBI, 2015). Fig. 7 illustrates Krevelen's diagram, combined with the half-life estimate proposed by Spokas (2010) based on laboratory-incubated synthetic biochars. The diagram shows that all biochars exhibit potential long-term persistence of several centuries or more, depending on experimental conditions. Biochars derived from cashew nut shells are distinguished by their ratio (O/Corg < 0.2), indicating a more stable, less biodegradable and less oxidised structure (Spokas, 2010). They are below the EBC threshold (O/Corg < 0.4), indicating strong carbon sequestration potential (EBC, 2022). The nature of the biomass, residence time, and, above all, temperature are factors that have been suggested as substitutes for stability (Baldock and Smernik, 2002).

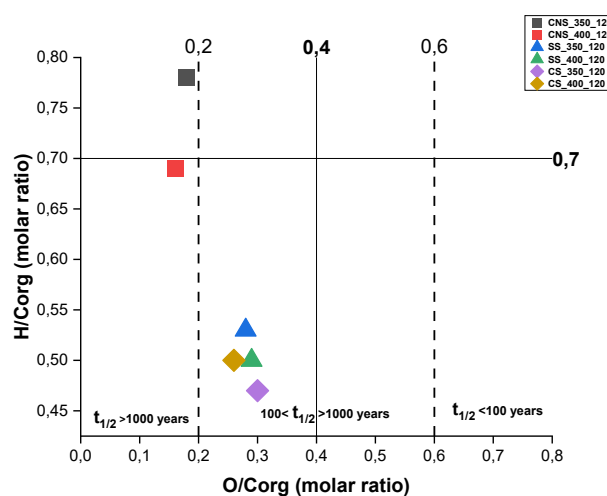


**Fig. 7.** Van Krevelen diagram

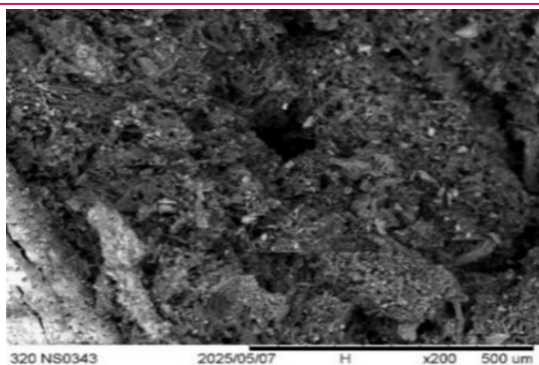


**Fig. 8.** SEM image of SS\_400\_120

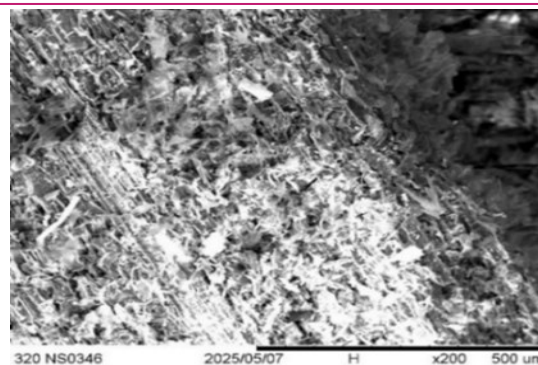


**Fig.9.** SEM image of CS\_400\_120

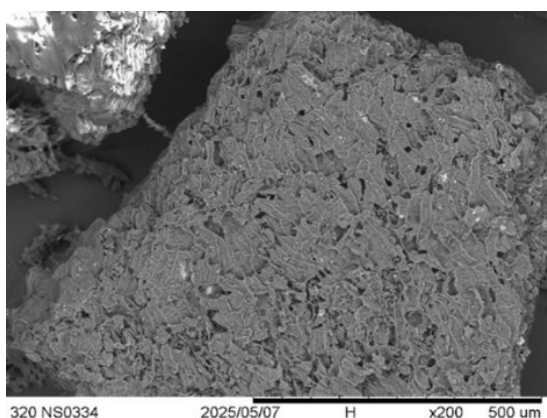


**Fig. 10.** SEM image of CNS\_400\_120

### Biochar morphology

Scanning electron microscopy (SEM) analysis enables the visualisation of the surfaces and porous structures of different biochars. A total of 12 biochars were subjected to SEM testing, as was the specific surface area. However, due to image quality, only the biochars with the highest specific surface area for each biomass, and for cashew nut shells with the lowest surface area ( $0.14 \text{ m}^2/\text{g}$ ), are presented, as shown in Fig. 8, 9, and 10. Fig. 8 shows the biochar produced from sorghum stalks and reveals a heterogeneous surface with visible aggregates and cavities (Downie *et al.*, 2009). This is characteristic of highly decomposed lignocellulosic materials (Ahmad *et al.*, 2014). This morphology is consistent with biochar produced at intermediate temperatures, representing a compromise between pore development and chemical stability (Zhao *et al.*, 2013). Unlike the biochar produced from sorghum stalks, the biochars produced from maize stalks in Fig. 9 have a more rectilinear and less fragmented structure. This organisation promotes porosity, which is conducive to water storage and nutrient retention. Fig. 10 shows a biochar with a compact, dense, low-porosity structure, typical of lignin-rich biomass-derived biochars. The CNS sample ( $0.14 \text{ m}^2/\text{g}$ ) shows lighter areas, which may indicate the presence of tar residues that could clog the cavities. This morphology results from advanced carbonisation, indi-

cating a relatively low specific surface area (Suliman *et al.*, 2016).

### Conclusion

This study characterised biochars produced from three abundant agricultural biomass sources in Togo: cashew nut shells, sorghum stalks and maize stalks. These biomasses were selected as representative agricultural and agro-industrial residues in order to assess the influence of carbonisation conditions on the properties and potential applications of biochar. The samples were obtained by slow carbonisation in a muffle furnace at two temperatures (350 and 400 °C) with holding times of 30, 60 and 120 minutes. Biochars derived from cashew nut shells had the highest yield and conductivity due to the rigidity of the shell and the presence of soluble salts. The pH levels of biochars derived from sorghum and maize stalks were the most alkaline. The low nitrogen content (0.6-1.6%) highlights the role of biochar as a soil conditioner rather than a fertiliser. The macronutrient and micronutrient content is highly dependent on biomass and temperature, suggesting differentiated agronomic potential. Spectroscopy (FTIR) reveals the emergence of aromatic bands for CNS-400\_120 and SS-350\_120, particularly for CNS-400\_120, as confirmed by the Krevelen diagram, thus complying with IBI and EBC standards. This shows that biochars derived from cashew nut shells are more effective for carbon sequestration, with the potential to persist for several centuries. Biochars derived from corn straw and sorghum had moderate apparent surface areas (28 to  $35.07 \text{ m}^2/\text{g}$ ). The moderate specific surface area ( $35.07 \text{ m}^2/\text{g}$ ) could indicate the presence of macropores conducive to water and nutrient retention, which is an additional agronomic advantage. These results highlight the potential of using biochars derived from cashew nut shells, sorghum and maize stalks as sustainable soil amendments. Although the total nutrient content has been quantified, the availability of nutrients under soil conditions remains to be evaluated. Future studies

should investigate nutrient leaching, mineralisation and bioavailability in order to better predict their agronomic potential.

## ACKNOWLEDGEMENTS

This research was supported by the Ministry of Higher Education and Research through the Support Project for Reform in Science and Engineering Education (PRSEE). The work was conducted in the laboratory at Kara University in Togo and the (E2Lim) laboratory at Limoges University in France. We express our sincere thanks to all those who contributed to the success of this project.

## Conflict of interest

The authors declare that they have no conflict of interest.

## REFERENCES

- Ahmad, M., Rajapaksha, A. U., Lim, J. E., Zhang, M., Bolan, N., Mohan, D., Vithanage, M., Lee, S. S. & Ok, Y. S. (2014). Biochar as a sorbent for contaminant management in soil and water: A review. *Chemosphere*, 99, 19-33.
- Allaire, Su. E. (2013). Le biochar dans les milieux poreux: Une solution miracle en environnement *Vecteur Environnement*.
- Araujo, Y.R.V., Souza, B.I. et & Carvalho, M. (2024). Greenhouse gas emissions associated with tree pruning residues of urban areas of Northeast Brazil, *Resources*, 13(9), p. 127.
- Ateş, F., Miskolczi, N. & Borsodi, N. (2013). Comparison of real waste (MSW and MPW) pyrolysis in batch reactor over different catalysts. Part I: Product yields, gas and pyrolysis oil properties. *Bioresource Technology*, 133, 443-454.
- Baldock, J. A. & Smernik, R. J. (2002). Chemical composition and bioavailability of thermally altered Pinus resinosa (Red pine) wood. *Organic Geochemistry*, 33(9), 1093-1109.
- Beesley, L., Moreno-Jiménez, E., Gomez-Eyles, J. L., Harris, E., Robinson, B. & Sizmur, T. (2011). A review of biochars' potential role in the remediation, revegetation and restoration of contaminated soils. *Environmental Pollution*, 159(12), 3269-3282.
- Breker, M.C. (2016). *Influence of amendments on chemical and biological properties of sodic soils*. North Dakota State University.
- Cantrell, K. B., Hunt, P. G., Uchimiya, M., Novak, J. M. & Ro, K. S. (2012). Impact of pyrolysis temperature and manure source on physicochemical characteristics of biochar. *Bioresource Technology*, 107, 419-428.
- Carrier, M., Hardie, A. G., Uras, Ü., Görgens, J. & Knoetze, J. H. (2012). Production of char from vacuum pyrolysis of South-African sugar cane bagasse and its characterisation as activated carbon and biochar. *Journal of Analytical and Applied Pyrolysis*, 96, 24-32.
- Chen, B., Chen, Z. & Lv, S. (2011). A novel magnetic biochar efficiently sorbs organic pollutants and phosphate. *Bioresource Technology*, 102(2), 716-723.
- Chen, Y., Yang, W., Zou, Y., Wu, Y., Mao, W., Zhang, J., Zia-ur-Rehman, M., Wang, B. & Wu, P. (2023). Quantification of the effect of biochar application on heavy metals in paddy systems: Impact, mechanisms and prospects. *Science of The Total Environment*, 168874.
- Chung, K.W.Y. *et al.* (2024) « Pyrolysis of cashew nut shells-focus on extractives », *Journal of Analytical and Applied Pyrolysis*, 179, p.106.
- Chou, B. (2015) « Analyse des propriétés de biochars ». [https://materiaux\\_renouvelables.ulaval.ca/wp-content/uploads/2015/05/Analyse\\_comparative\\_biochar\\_fomat.pdf](https://materiaux_renouvelables.ulaval.ca/wp-content/uploads/2015/05/Analyse_comparative_biochar_fomat.pdf)
- Cruz, T., Maranon, A., Hernandez, C., Alvarez, O., Ayala-García, C. & Porras, A. (2024). Exploring the potential of cashew nutshells: A critical review of alternative applications. *BioResources*, 19(3), 6768.
- Dabin, B. (1965). Dosage de l'azote total dans les sols par la methode de Kjeldahl. *Cahiers Office de la Recherche Scientifique et Technique Outre-Mer, Serie Pedologie*, 3, 338-348.
- Di Blasi, C. (2008) « Modeling chemical and physical processes of wood and biomass pyrolysis », *Progress in Energy and Combustion Science*, 34(1), p. 47-90.
- Downie, A., Crosky, A. & Munroe, P. (2009). Physical properties of biochar, biochar for environmental management science and technology. *Earthscan, London*.
- EBC (2022). *European Biochar Certificate—Guidelines for a Sustainable production of biochar Version 10.1*. European Biochar Foundation (EBC), Arbaz, Switzerland. (<http://european-biochar.org>).
- Enders, A., Hanley, K., Whitman, T., Joseph, S. & Lehmann, J. (2012). Characterization of biochars to evaluate recalcitrance and agronomic performance. *Bioresource Technology*, 114, 644-653.
- Evans, M.R. *et al.* (2017) « Chemical properties of biochar materials manufactured from agricultural products common to the Southeast United States ».
- Fuertes, A. B., Arbestain, M. C., Sevilla, M., Maciá-Agulló, J. A., Fiol, S., López, R., Smernik, R. J., Aitkenhead, W. P., Arce, F. & Macías, F. (2010). Chemical and structural properties of carbonaceous products obtained by pyrolysis and hydrothermal carbonisation of corn stover. *Soil Research*, 48(7), 618-626.
- Gaskin, J., Steiner, C., Harris, K., Das, K. C. & Bibens, B. (2008). Effect of low-temperature pyrolysis conditions on biochar for agricultural use. *Transactions of the ASABE*, 51(6), 2061-2069.
- Glaser, B., Lehmann, J. & Zech, W. (2002). Ameliorating physical and chemical properties of highly weathered soils in the tropics with charcoal—a review. *Biology and Fertility of Soils*, 35(4), 219-230.
- Godjo, T. (2017). Densification and analysis of the physical properties of bio-coal produced from the pyrolysis cashew nut shells in Benin. *International Journal of Innovation and Applied Studies*, 19(3), 614.
- Godjo, T., Tagutchou, J.-P., Naquin, P. & Gourdon, R. (2015). Valorisation des coques d'anacarde par pyrolyse au Bénin. *Environnement, Ingénierie & Développement*.
- Hwang, N. & Barron, A. R. (2011). BET surface area

- analysis of nanoparticles. *The Connexions Project*
27. Hsu, C.-P. S. (1997). Infrared spectroscopy. Handbook of instrumental techniques for analytical chemistry, 249.
  28. IBI (2015). *Specification Standards : Standardized Product Definition and Product Testing Guidelines for Biochar That Is Used in Soil (aka IBI Biochar Standards)*.
  29. Jindo, K., Mizumoto, H., Sawada, Y., Sanchez-Monedero, M. A. & Sonoki, T. (2014a). Physical and chemical characterization of biochars derived from different agricultural residues. *Biogeosciences*, 11(23), 6613-6621.
  30. Jindo, K., Mizumoto, H., Sawada, Y., Sanchez-Monedero, M. A. & Sonoki, T. (2014b). Physical and chemical characterizations of biochars derived from different agricultural residues. *Biogeochemistry: Organic Biogeochemistry*. <https://doi.org/10.5194/bgd-11-11727-2014>
  31. Joseph, S. (2012). *Biochar for environmental management: Science and Technology*. Routledge.
  32. Joseph, U. E., Toluwase, A. O., Kehinde, E. O., Omasan, E. E., Tolulope, A. Y., George, O. O., Zhao, C. & Hongyan, W. (2020). Effect of biochar on soil structure and storage of soil organic carbon and nitrogen in the aggregate fractions of an Albic soil. *Archives of Agronomy and Soil Science*, 66(1), 1-12. <https://doi.org/10.1080/03650340.2019.1587412>
  33. Kadjo, B. S., Sako, M. K., Diango, K. A., Danlos, A. & Perilhon, C. (2024). Characterization and optimization of the heat treatment of cashew nutshells to produce a biofuel with a high-energy value. *AIMS Energy*, 12(2).
  34. Khater, E. S., Bahnasawy, A., Hamouda, R., Sabahy, A., Abbas, W. & Morsy, O. M. (2024). Biochar production under different pyrolysis temperatures with different types of agricultural wastes. *Scientific Reports*, 14(1), 2625.
  35. Keiluweit, M., Nico, P. S., Johnson, M. G. & Kleber, M. (2010a). Dynamic molecular structure of plant biomass-derived black carbon (Biochar). *Environmental Science & Technology*, 44(4), 1247-1253. <https://doi.org/10.1021/es9031419>
  36. Kuligiewicz, A., Derkowski, A., Szczerba, M., Gionis, V. & Chryssikos, G. D. (2015). Revisiting the infrared spectrum of the water—Smectite interface. *Clays and Clay Minerals*, 63(1), 15-29.
  37. Kumar, N., Ponnuswami, V., Jeeva, S., Ravindran, C. & Kalaivanan, D. (2012). Cashew Industry in India—an overview. *Chronica Horticulturae*, 52(1), 27.
  38. Kwapinski, W., Byrne, C. M. P., Kryachko, E., Wolfram, P., Adley, C., Leahy, J. J., Novotny, E. H. & Hayes, M. H. B. (2010). Biochar from biomass and waste. *Waste and Biomass Valorization*, 1(2), 177-189. <https://doi.org/10.1007/s12649-010-9024-8>
  39. Lehmann, J. (2007). Bio-energy in the black. *Frontiers in Ecology and the Environment*, 5(7), 381-387. [https://doi.org/10.1890/1540-9295\(2007\)5%255B381:BITB%255D2.0.CO](https://doi.org/10.1890/1540-9295(2007)5%255B381:BITB%255D2.0.CO)
  40. Lehmann, J., Gaunt, J. & Rondon, M. (2006). Bio-char sequestration in terrestrial ecosystems—a review. Mitigation and adaptation strategies for global change, 11, 403-427.
  41. Lehmann, J. & Joseph, S. (2015). Biochar for environmental management : An introduction. In *Biochar for Environmental Management*, (p. 1-13). Routledge.
  42. Lehmann, J., Rillig, M. C., Thies, J., Masiello, C. A., Hockaday, W. C. & Crowley, D. (2011). Biochar effects on soil biota—a review. *Soil Biology and Biochemistry*, 43(9), 1812-1836.
  43. Leng, Z., Padhan, R.K. et & Sreeram, A. (2018) « Production of a sustainable paving material through chemical recycling of waste PET into crumb rubber modified asphalt », *Journal of Cleaner Production*, 180, p. 682-688.
  44. McCall, M. A., Watson, J. S., Tan, J. S. W. & Sephton, M. A. (2025). Biochar stability revealed by FTIR and machine learning. *ACS Sustainable Resource Management*, 2(5), 842-852. <https://doi.org/10.1021/acssusres.mgt.5c00104>
  45. McIntosh, C. & Hunt, J. (2013). *Biochar + compost (technical white paper)*. Pacific biochar benefit corporation, United States
  46. McKinley, B. A., Olson, S. N., Ritter, K. B., Herb, D. W., Karlen, S. D., Lu, F., Ralph, J., Rooney, W. L. & Mullet, J. E. (2018). Variation in energy sorghum hybrid biomass composition and lignin chemistry during development under irrigated and non-irrigated field conditions. *PLoS One*, 13(4), e0195863.
  47. Mohan, D., Pittman Jr, C. U. & Steele, P. H. (2006). Pyrolysis of wood/biomass for bio-oil : A critical review. *Energy & Fuels*, 20(3), 848-889.
  48. Mukherjee, A., Lal, R. & Zimmerman, A. R. (2014). Effects of biochar and other amendments on the physical properties and greenhouse gas emissions of an artificially degraded soil. *Science of the Total Environment*, 487, 26-36.
  49. Mukherjee, A., Patra, B. R., Podder, J. & Dalai, A. K. (2022). Synthesis of biochar from lignocellulosic biomass for diverse industrial applications and energy harvesting : Effects of pyrolysis conditions on the physicochemical properties of biochar. *Frontiers in Materials*, 9. <https://doi.org/10.3389/fmats.2022.870184>
  50. Nguyen, L. X., P. D. & Miyanishi, T. (2018). Properties of biochars prepared from local biomass in the mekong delta, Vietnam. *BioResources*, 13(4), 7325-7344. <https://doi.org/10.15376/biores.13.4.7325-7344>
  51. Nicholas, H. L., Mabbett, I., Apsey, H. & Robertson, I. (2022). Physico-chemical properties of waste-derived biochar from community-scale faecal sludge treatment plants. *Gates Open Research*, 6, 96.
  52. Novak, J. M., Lima, I., Xing, B., Gaskin, J. W., Steiner, C., Das, K. C., Ahmedna, M., Rehrh, D., Watts, D. W. & Busscher, W. J. (2009). Characterization of designer biochar produced at different temperatures and their effects on a loamy sand. *Annals of Environmental Science*.
  53. Parikh, S. J., Goynes, K. W., Margenot, A. J., Mukome, F. N. D. & Calderón, F. J. (2014). Soil chemical insights provided through vibrational spectroscopy. In *Advances in Agronomy* (126, 1-148). Elsevier. <https://doi.org/10.1016/B978-0-12-800132-5.00001-8>
  54. Parmakoğlu, Emire Ülkü, Ahmet Çay & Jale Yanık. (2023). Valorization of Solid 177/24723444221147983, 10, 3, 133-143.
  55. Phillips, C. L., Meyer, K. M., Garcia-Jaramillo, M.,

- Weidman, C. S., Stewart, C. E., Wanzek, T., ... & Trippe, K. M. (2022). Towards predicting biochar impacts on plant-available soil nitrogen content. *Biochar*, 4(1), 9.
56. Qian, L. & Chen, B. (2013). Dual role of biochars as adsorbents for aluminum: The effects of oxygen-containing organic components and the scattering of silicate particles. *Environmental Science & Technology*, 47(15), 8759-8768.
57. Rehrah, D., Reddy, M. R., Novak, J. M., Bansode, R. R., Schimmel, K. A., Yu, J., Watts, D. W. & Ahmedna, M. (2014). Production and characterization of biochars from agricultural by-products for use in soil quality enhancement. *Journal of Analytical and Applied Pyrolysis*, 108, 301-309.
58. Robertson, S. J., Rutherford, P. M., López-Gutiérrez, J. C. & Massicotte, H. B. (2012). Biochar enhances seedling growth and alters root symbioses and properties of sub-boreal forest soils. *Canadian Journal of Soil Science*, 92(2), 329-340. <https://doi.org/10.4141/cjss2011-066>
59. Rutherford, D. W., Wershaw, R. L., Rostad, C. E. & Kelly, C. N. (2012). Effect of formation conditions on biochars: Compositional and structural properties of cellulose, lignin, and pine biochars. *Biomass and Bioenergy*, 46, 693-701.
60. Singh, B., Camps-Arbestain, M. & Lehmann, J. (2017). *Biochar: A Guide to Analytical Methods*. Csiro Publishing.
61. Spokas, K. A. (2010a). Review of the stability of biochar in soils: Predictability of O: C molar ratios. *Carbon Management*, 1(2), 289-303.
62. Spokas, K. A. (2010b). Review of the stability of biochar in soils: Predictability of O:C molar ratios. *Carbon Management*, 1(2), 289-303. <https://doi.org/10.4155/cmt.10.32>
63. Suliman, W., Harsh, J. B., Abu-Lail, N. I., Fortuna, A.-M., Dallmeyer, I. & Garcia-Perez, M. (2016). Influence of feedstock source and pyrolysis temperature on biochar bulk and surface properties. *Biomass and Bioenergy*, 84, 37-48.
64. Tomczyk, A., Sokołowska, Z. & Boguta, P. (2020). Biochar physicochemical properties: Pyrolysis temperature and feedstock kind effects. *Reviews in Environmental Science and Bio/Technology*, 19(1), 191-215.
65. Tripathi, M., Sahu, J. N. & Ganesan, P. (2016). Effect of process parameters on production of biochar from biomass waste through pyrolysis: A review. *Renewable and Sustainable Energy Reviews*, 55, 467-481.
66. Van Zwieten, L. *et al.* (2010). Effects of biochar from slow pyrolysis of papermill waste on agronomic performance and soil fertility », *Plant and Soil*, 327(1), p. 235-246.
67. Vassilev, S. V., Baxter, D., Andersen, L. K. & Vassileva, C. G. (2013). An overview of the composition and application of biomass ash. : Part 2. Potential utilisation, technological and ecological advantages and challenges. *Fuel*, 105, 19-39.
68. Xie, T., Reddy, K. R., Wang, C., Yargicoglu, E. & Spokas, K. (2015). Characteristics and applications of biochar for environmental remediation: A review. *Critical Reviews in Environmental Science and Technology*, 45 (9), 939-969. <https://doi.org/10.1080/10643389.2014.924180>
69. Yang, H., Yan, R., Chen, H., Lee, D. H. & Zheng, C. (2007). Characteristics of hemicellulose, cellulose and lignin pyrolysis. *Fuel*, 86(12-13), 1781-1788.
70. Zabaleta, A. J., Mercado, T., Marrugo, J. L. & Diaz, J. J. F. (2018). Curve Number (CN) as Pressure Indicator of the Hydrological Condition under Global Warming Scenarios at a Local Scale in La Mojana Region, Colombia. *Indian Journal of Science and Technology*, 1-12.
71. Zhao, L., Cao, X., Mašek, O. & Zimmerman, A. (2013). Heterogeneity of biochar properties as a function of feedstock sources and production temperatures. *Journal of Hazardous Materials*, 256, 1-9.
72. Zhao, Q., Cui, J., Hou, Y. & Pei, P. (2024). Effect of pyrolysis temperature on physicochemical characteristics and toxic elements for grub manure-derived biochar. *RSC Advances*, 14(38), 27883-27893.